5.6. Barrow, Alaska (01/14/12 – 11/28/12)

This section describes quality control of solar data recorded at Barrow between 01/14/12 – 11/28/12. No site visit was performed during this period. A total of 8,522 SUV scans are part of the Barrow Volume 22 dataset.

Data collected during the reporting period are affected by the following problems:

- Reduced duty cycle
  The shutter of the SUV-100 became "sticky" at the end of the winter and there was the risk that it would not fully open during solar scans. The system's duty cycle was therefore reduced from four to two scans per hour.
- Partial failure of shutter and resulting loss of data
  The shutter did not open completely between 7/12/12 and 7/30/12. Measurements of solar irradiance were therefore too small. The magnitude of the bias was too variable to apply a correction. Data of this period were excluded from the published data set. A new shutter is currently being developed and will be installed at the beginning of 2013. This system upgraded is expected to prevent any shutter-related data loss in the future.

5.6.1. Irradiance Calibration

The site irradiance standards of the reporting period were the lamps M-699, 200W009, and 200W042.

Lamp 200W042 was calibrated in June 2007 at BSI with four 1000-Watt FEL lamps provided by the Central UV Calibration Facility (CUCF) at Boulder. This calibration procedure was complicated by the fact that the irradiance scale of the four FEL lamps refers to the detector-based scale of the National Institute of Standards and Technology established in 2000 (NIST2000; Yoon et al., 2002), whereas all solar data of the NSF UVSIMN refer to the source-based NIST scale from 1990 (NIST1990, Walker et al., 1987). The NIST2000 scale is about 1.3% larger than the NIST1990 scale. Data of certificates issued by CUCF were converted to the NIST1990 scale before the calibration was transferred to the site standard.

Lamps M-699 and 200W009 were originally calibrated by Optronic Laboratories (OL) in March 2001. Both lamps were brought to San Diego in 2007 and recalibrated against lamps 200W028 and 200W022. (Lamp 200W028 is the San Diego site standard; lamp 200W022 is BSI's long-term standard, which preserves the OL scale from March 2001.)

The three lamps were compared to the traveling standard 200W017 in March 2010. At this time, the calibrations of the lamps agreed with that of 200W017 to within ±1.5%. (The calibration of lamp 200W017 is traceable to the NIST1990 scale in the same way as lamp 200W042.)

The three site standards were compared with each other on 02/12/12, 7/11/12, 8/19/12, 9/29/12, and 11/18/12. The lamps agreed to within ±1.5% on all occasions, giving confidence in the scale of irradiance represented by the lamps. Figure 5.6.1 shows as an example the comparison performed on 7/11/12.

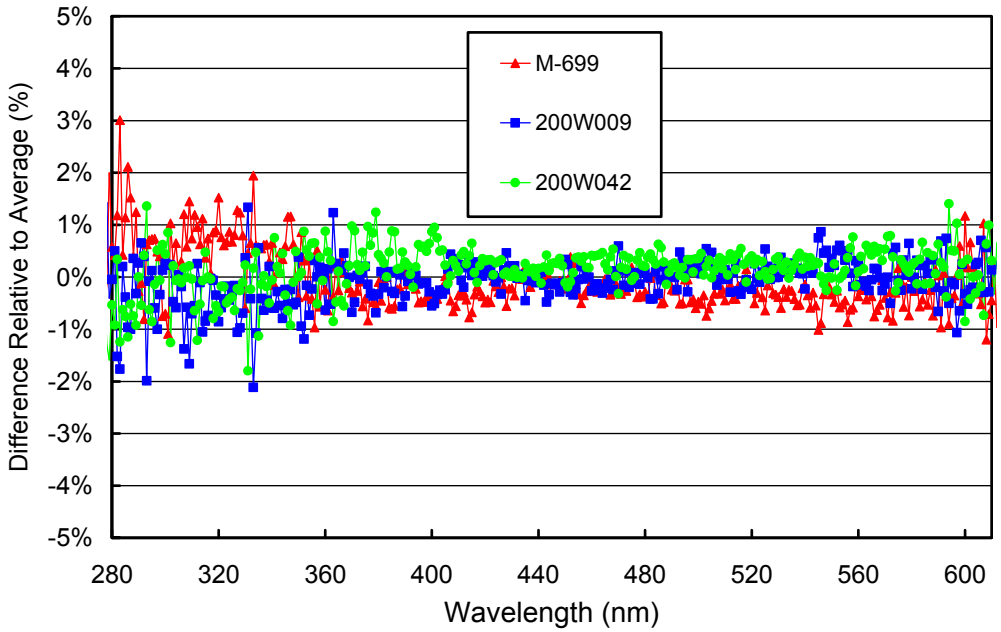

Figure 5.6.1. *Comparison of on-site lamps M-699, 200W009, and 200W042 on 7/11/12.*

5.6.2. Instrument Stability and Calibration

The radiometric stability of the SUV-100 spectroradiometer was monitored with calibrations utilizing the three site irradiance standards, daily "response" scans of the internal lamp, by comparison with measurements of the GUV-511 multifilter radiometer, and by comparisons with results of a radiative transfer model.

The stability of the internal lamp is monitored with the TSI sensor, which is independent from possible monochromator and PMT drifts. By logging the PMT currents at several wavelengths during response scans, changes in monochromator throughput and PMT sensitivity can be detected. Figure 5.6.2 shows changes in TSI readings and PMT currents at 300 and 400 nm, derived from all response scans performed in 2012. TSI measurements indicate that the internal lamp became darker by about 1.5% over time. The PMT current at 400 nm tracks the TSI measurement very well, indicating excellent stability of monochromator throughput and PMT sensitivity. The variation of the PMT current at 300 nm shows a somewhat larger amplitude than that at 400 nm because changes in a lamp's spectral irradiance tend to be larger at shorter wavelengths.

Through-the-collector calibrations using the site irradiance standards indicated a somewhat larger variability in system responsivity than that indicated by monitoring the internal lamp. To adjust for these small changes, the reporting period was subdivided into six periods. Figure 5.6.3 shows the ratio of the irradiance assigned to the internal reference lamp in Periods P2 - P6 relative to that applied in Period P1. Table 1 provides more information on these periods. The change in responsivity over the year was less than ±3% at all wavelengths. There is no clear trend in the direction of the responsivity change.

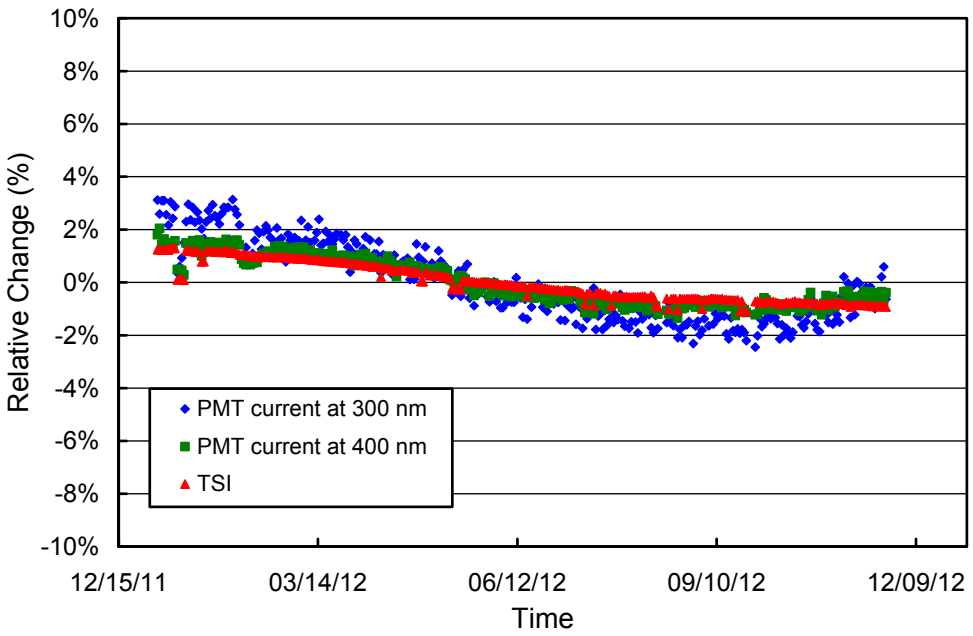

Figure 5.6.2. *Time-series of PMT current at 300 and 400 nm, and TSI signal extracted from measurements of the internal irradiance standard at Barrow. All data sets are normalized to their average.*

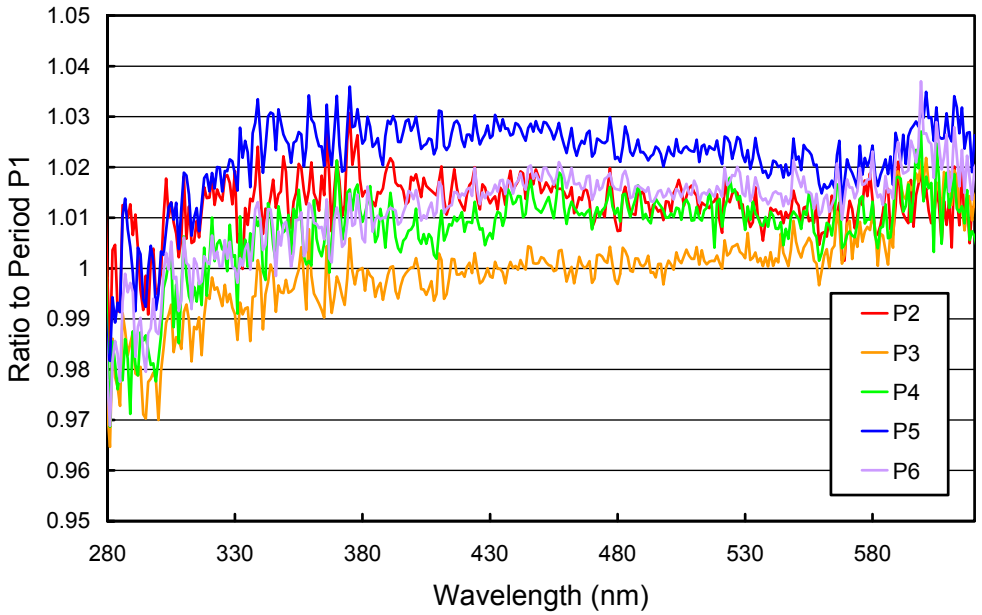

Figure 5.6.3. *Ratios of spectral irradiance assigned to the internal reference lamp during the Periods P2-P6 relative to Period P1.*

Table 5.6.1. Calibration periods for Barrow Volumes 22.

Period name	Period range	Number of absolute scans
P1	01/01/12 - 01/30/12	2
P2	01/31/12 - 02/12/12	2
P3	02/13/12 - 04/22/12	4
P4	04/23/12 - 05/16/12	2
P5	05/17/12 - 07/20/12	6
P6	07/21/12 - 12/31/12	8

Figure 5.6.4 presents ratios of standard deviation and average spectra, calculated from individual absolute scans performed in each calibration period. These ratios are useful for estimating the variability of calibrations assigned to each period. The variability is less than 1.5% for all periods. Period P6 originally also included three additional absolute scans that did not agree well with the rest of the scans for unknown reasons. These scans were not used when calculating the calibration file for this period. The effect of these scans on the relative standard deviation spectra shown in Figure 5.6.4 was calculated and the result is indicated by the broken line in this figure.

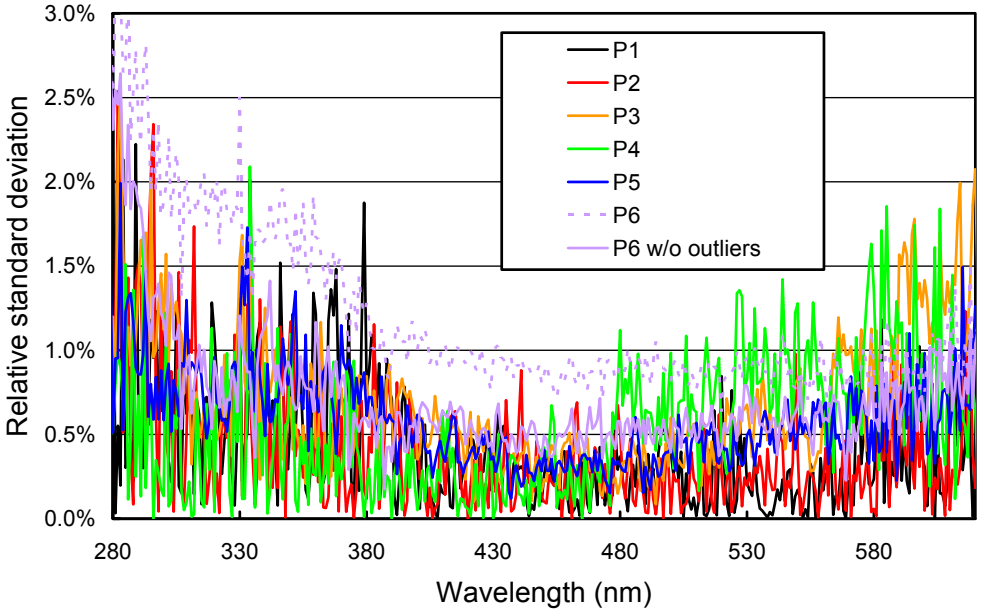

Figure 5.6.4. *Ratio of standard deviation and average spectra calculated from irradiance spectra applied to the internal lamp.*

SUV-100 data were also compared to measurements of the collocated GUV-511 radiometer. The ratio of GUV and SUV data at 340 nm as a function of time is shown in Figure 5.6.5. The standard deviation of the ratio is 0.038. Variability is generally smaller in spring than fall (e.g., Period P6) because of less influence by clouds. The GUV/SUV ratio shows several step changes and short periods with systematic (i.e., non-random) difference from one. The most obvious step change is the one marked with "A" in Figure 5.6.5. Closer inspection did not reveal the cause for this step change, which is about 4% in magnitude. For example, the ratio of TSI measurements and SUV measurement weighted with the response function of the TSI was stable over the period in question, suggesting that SUV measurements are not the cause of the step change. Comparisons between SUV measurements and radiative transfer calculations also did not indicate

a sudden change in the SUV's sensitivity. SUV calibrations of period P3 were consistent (Figure 5.6.4.), indicating again that SUV data are not to blame. While this analysis points to the GUV radiometer as the source of the discontinuity, inspection of the GUV data did not corroborate this suspicion. The cause of the step change is therefore unclear.

The GUV/SUV ratio was relative high on 6/23/12 and 6/24/12 ("B" in Figure 5.6.5). During the same period the ratio of TSI and SUV measurement weighted with the response function of the TSI were abnormally low. This is an indication that SUV data could be a few percent too small during this period. Likewise, the GUV/SUV ratio was relative high between 7/6/12 and 7/11/12 ("C" in Figure 5.6.5). TSI measurements during this period were within the norm. However, comparisons with the model suggest that SUV measurements were about 4% too low during this period, consistent with the GUV/SUV ratio.

Between 7/12/12 and 7/30/12, the shutter of the SUV did not open completely. Measured data were too small. The magnitude of the bias was too variable to apply a correction. Data of this period were therefore excluded from the published data set. It is possible that SUV data measured immediately before this period (that is the period marked with "C" in Figure 5.6.5) were already somewhat affected by the problem. This would explain the relatively high GUV/SUV ratio of this period.

Some abnormally large values of the GUV/SUV ratio were also observed for the following periods: 04/06/12 21:00 - 04/07/12 06:30, 05/02/12 11:30 - 05/02/12 14:00, and 09/27/12 16:30 - 09/27/12 20:30. Data of this period were flagged in the Version 2 data edition.

The variability of the GUV/SUV ratio is relatively high in Period 6. Similar variation between the measurements of the two instruments has also been observed in previous years. Some of the variation stems from the low radiation levels and small solar elevation during the period. For example, the GUV/SUV ratio always tends to be below one in October. However, it is possible that a part of the variability is caused by incomplete opening of the shutter. The uncertainty of measurements in Period P6 is therefore somewhat higher than the uncertainty discussed by *Bernhard et al*. [2007].

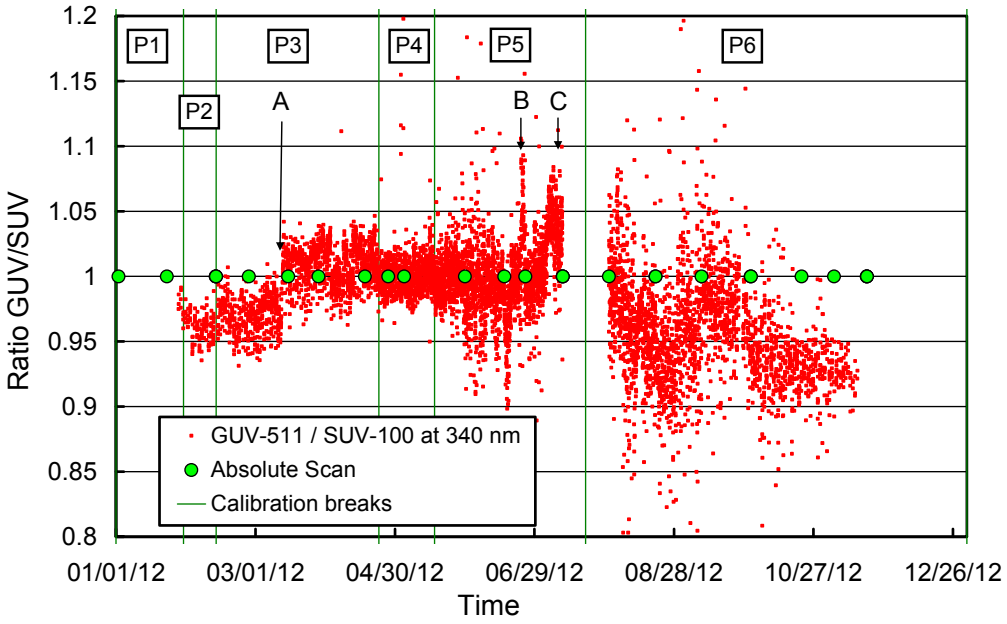

Figure 5.6.5. *Ratio of GUV-511 measurements of the 340-nm channel to SUV-100 measurements. The latter were weighted with the spectral response function of the 340-nm GUV-511 channel. Times of absolute scans and calibration breaks are also indicated. The features marked with "A", "B", and "C" are discussed in the text.*

As a last check of data quality, SUV-100 measurements were compared with radiative transfer calculations. These calculations are part of Version 2 processing (www.biospherical.com/NSF/Version2/). The ratio of measured and modeled data was generally within the range observed in past years with the exception of the short periods discussed above (e.g., 6/23/12 and 6/24/12, and 7/6/12 - 7/11/12).

5.6.3. Wavelength Calibration

Wavelength stability of the system was monitored with the internal mercury lamp. Information from the daily wavelength scans was used to homogenize the data set by correcting day-to-day fluctuations in the wavelength offset. Figure 5.6.6 shows the differences in the wavelength offset of the 296.73 nm mercury line between two consecutive wavelength scans. A total 359 pairs, measured between 1/1/12 and 11/28/12, were evaluated and the change in offset was smaller than ±0.03 nm in all cases.

The function for correcting the non-linearity of the monochromator's wavelength drive is shown in Figure 5.6.7. The function was calculated with the Version 2 Fraunhofer line correlation method (*Bernhard et al*., 2004). Data were corrected with these functions and again tested with the correlation method. Results for four wavelengths in the UV and one in the visible are shown in Figure 5.6.8. Residual shifts in the UV are typically smaller than ±0.05 nm. The average standard variation for all wavelengths between 310 and 590 nm is 0.022 nm. Wavelength errors have been further reduced in the Version 2 data set.

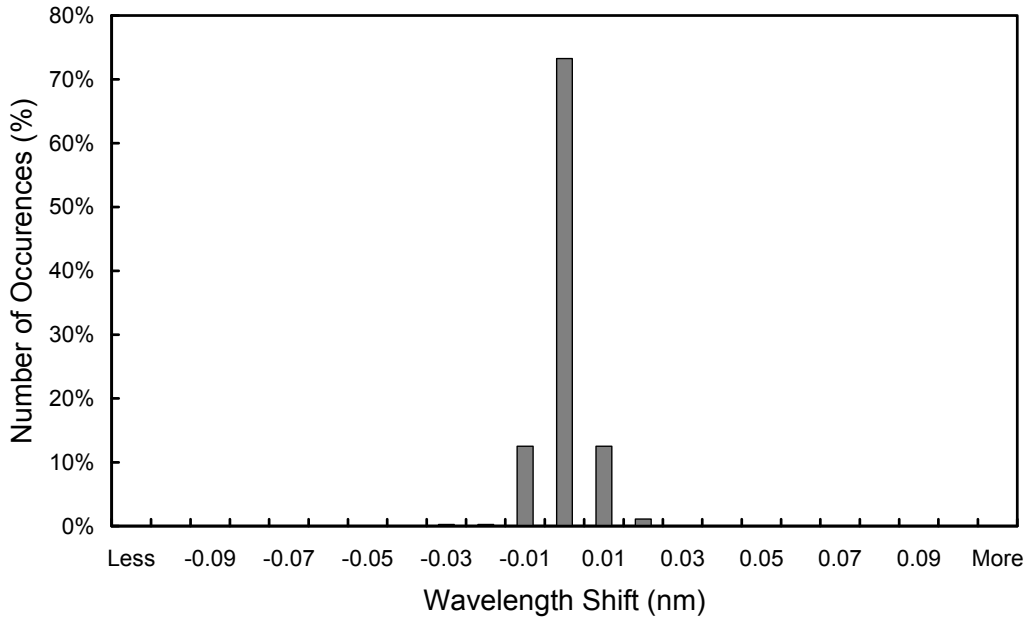

Figure 5.6.6. *Differences in the measured position of the 296.73 nm mercury line between consecutive wavelength scans. The x-labels give the center wavelength shift for each column. Thus the 0-nm histogram column covers the range -0.005 to +0.005 nm. "Less" means shifts smaller than –0.105 nm; "more" means shifts larger than 0.105 nm.*

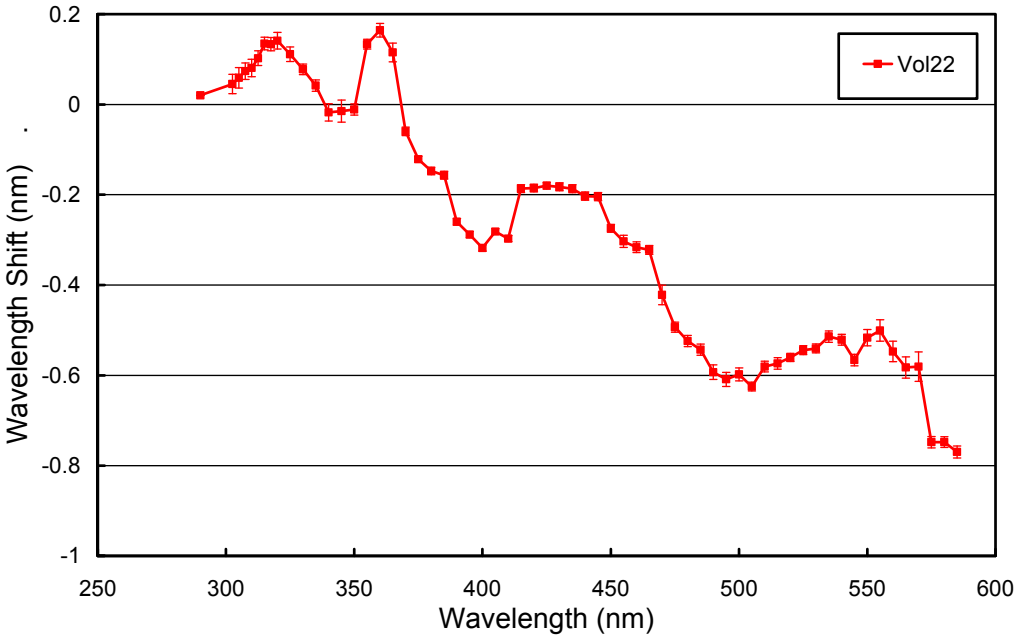

Figure 5.6.7. *Monochromator non-linearity correction functions for Barrow Volume 22. Error bars indicate the standard deviation of the data contributing to this plot.*

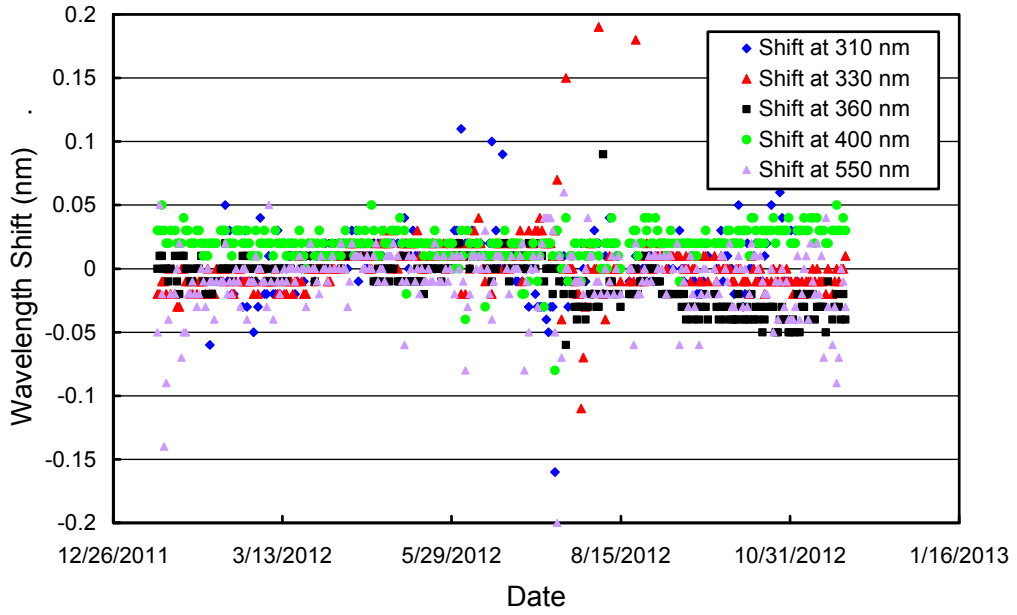

Figure 5.6.8. *Wavelength accuracy check of final data at four wavelengths in the UV and one in the visible by means of Fraunhofer-line correlation. The noontime measurement has been evaluated for each day of the reporting period when the Sun was above the horizon.*

5.6.4. Missing Data

A total of 8,522 scans are part of the Barrow Volume 22 dataset (01/14/12 – 11/28/12). There are no data for the following periods:

- 02/21/12: Shutter did not open completely (loss of 6 scans)
- 07/11/12 - 07/30/12: Shutter did not open completely (loss of 888 scans)

5.6.5. GUV Data

The GUV-511 radiometer installed next to the SUV-100 was calibrated against final SUV-100 measurements following the procedure outlined in Section 4.3.1. Data products were calculated from calibrated measurements (Section 4.3.2). Figure 5.6.9. shows a comparison of SUV-100 and GUV-511 erythemal irradiance based on final Volume 22 data. The bias between the two instruments depends somewhat on season. Some of the seasonality is caused by the simplifications of the GUV inversion procedure. Measurements of the GUV's 305 nm channel are close to the detection limit when SZA exceeds 75° and the total ozone column is large. The large noise in GUV data during those conditions also affects the calculation of secondary data products such as erythemal irradiance. We advise data users to use SUV-100 rather than GUV-511 data, in particular when the SZA exceeds 75°. GUV data can be used to "fill in" measurements of the SUV-100 in July when there are no data because of the shutter problem discussed above. The ratio of SUV and GUV is abnormally small between 4/6/12 21:30 and 4/7/12 02:30. SUV data of this period are likely too low. Version 2 data of this period have been flagged accordingly.

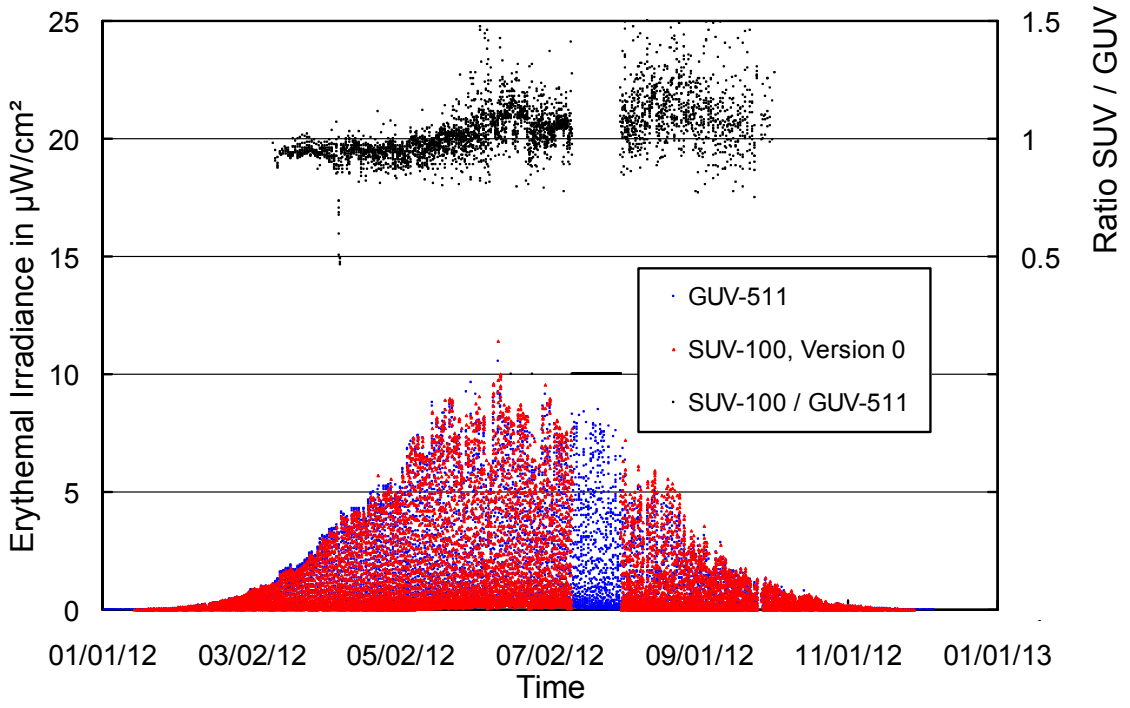

Figure 5.6.9. *Comparison of erythemal irradiance measured by the SUV-100 spectroradiometer and the GUV-511 radiometer. Data are based on "Version 0" (cosine-error uncorrected) data.*

Figure 5.6.10 shows a comparison of total ozone measurements from the GUV-511, the Ozone Monitoring Instrument (OMI) on NASA's AURA satellite (Version 8.5, Collection 3), and the SUV-100 (Version 2 data using climatological profiles with temperature correction). GUV-511 ozone values were calculated as described in Section 4.3.3. GUV-511 data measured between 3/12/12 and 4/14/12 are on average 3.2% smaller than OMI measurements. Between 4/15/12 and 9/30/12, GUV data are on average 2.1% larger. A

similar patterns was also observed in previous years. For SZAs larger than 75°, GUV-511 ozone data become unreliable and should not be used. SUV-100 ozone data exceed OMI measurements on average by 2.5%. For more information on total ozone calculation from SUV-data at Barrow see *Bernhard et al*., 2003. The effect of the vertical distribution of ozone has been further discussed by *Bernhard et al*. (2005).

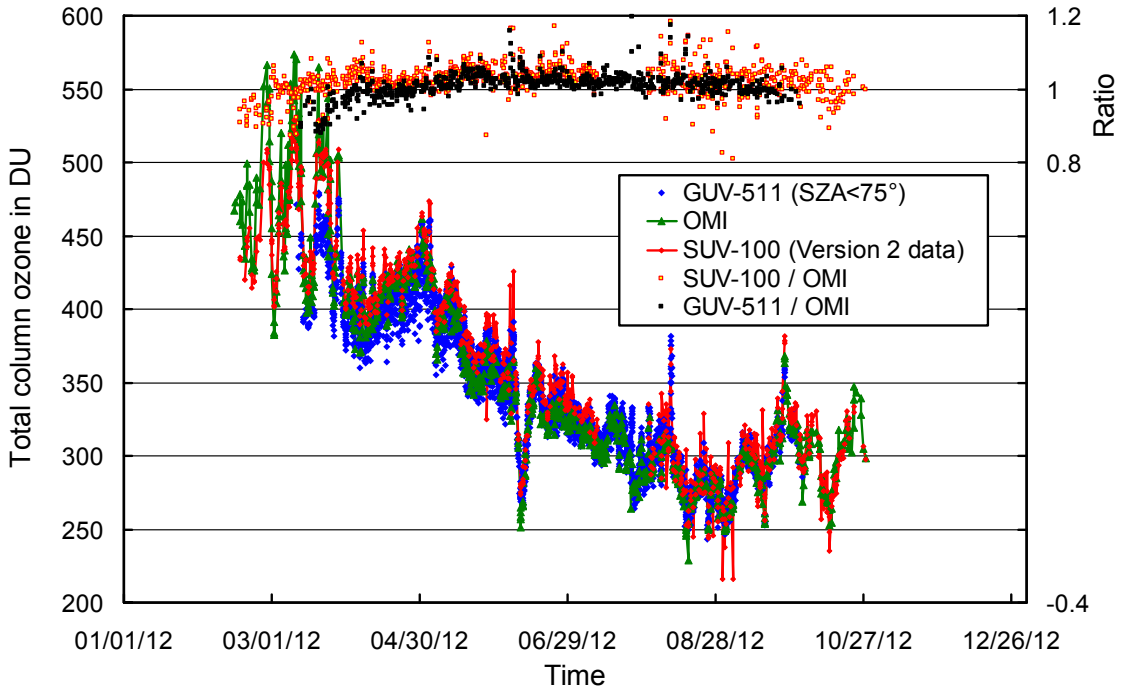

Figure 5.6.10. *Comparison of total column ozone measurements from GUV-511, OMI, and SUV-100. GUV-511 measurements are plotted in 30 minute intervals. For calculating the ratios of SUV-100/OMI and GUV-511/OMI, only measurements concurrent with the OMI overpass were evaluated.*

References

Bernhard, G., C.R. Booth, and R.D. McPeters. (2003). Calculation of total column ozone from global UV spectra at high latitudes. J. Geophys Research, 108(D17), 4532, doi:10.1029/2003JD003450.

Bernhard, G., C. R. Booth, and J. C. Ehramjian. (2004). Version 2 data of the National Science Foundation's Ultraviolet Radiation Monitoring Network: South Pole, J. Geophys. Res., 109, D21207, doi:10.1029/2004JD004937.

Bernhard, G., R.D. Evans, G.J. Labow, and S.J. Oltmans. (2005). Bias in Dobson Total Ozone Measurements at High Latitudes due to Approximations in Calculations of Ozone Absorption Coefficients and Airmass. J. Geophys. Res., 110, D10305, doi:10.1029/2004JD005559.

Bernhard, G., C. R. Booth, J. C. Ehramjian, R. Stone, and E. G. Dutton. (2007), Ultraviolet and visible radiation at Barrow, Alaska: Climatology and influencing factors on the basis of version 2 National Science Foundation network data, J. Geophys. Res., 112, D09101, doi:10.1029/2006JD007865.